Neurobiology of Disease

The Y99C Mutation in Guanylyl Cyclase-Activating Protein 1 Increases Intracellular Ca^{2+} and Causes Photoreceptor Degeneration in Transgenic Mice

Elena V. Olshevskaya,[1]* Peter D. Calvert,[2]* Michael L. Woodruff,[3]* Igor V. Peshenko,[1] Andrey B. Savchenko,[1] Clint L. Makino,[2] Ye-Shih Ho,[5] Gordon L. Fain,[3,4] and Alexander M. Dizhoor[1]

[1]Hafter Research Laboratories, Pennsylvania College of Optometry, Elkins Park, Pennsylvania 19027, [2]Department of Ophthalmology, Massachusetts Eye and Ear Infirmary, Harvard Medical School, Boston, Massachusetts 02114, [3]Department of Physiological Science and [4]Jules Stein Eye Institute, University of California at Los Angeles, Los Angeles, California 90095, and [5]Institute of Environmental Health Sciences, Wayne State University, Detroit, Michigan 48202

Guanylyl cyclase-activating proteins (GCAPs) are Ca^{2+}-binding proteins that activate guanylyl cyclase when free Ca^{2+} concentrations in retinal rods and cones fall after illumination and inhibit the cyclase when free Ca^{2+} reaches its resting level in the dark. Several forms of retinal dystrophy are caused by mutations in *GUCA1A*, the gene coding for GCAP1. To investigate the cellular mechanisms affected by the diseased state, we created transgenic mice that express GCAP1 with a Tyr99Cys substitution (Y99C GCAP1) found in human patients with a late-onset retinal dystrophy (Payne et al., 1998). Y99C GCAP1 shifted the Ca^{2+} sensitivity of the guanylyl cyclase in photoreceptors, keeping it partially active at 250 nM free Ca^{2+}, the normal resting Ca^{2+} concentration in darkness. The enhanced activity of the cyclase in the dark increased cyclic nucleotide-gated channel activity and elevated the rod outer segment Ca^{2+} concentration in darkness, measured by using fluo-5F and laser spot microscopy. In different lines of transgenic mice the magnitude of this effect rose with the Y99C GCAP1 expression. Surprisingly, there was little change in the rod photoresponse, indicating that dynamic Ca^{2+}-dependent regulation of cGMP synthesis was preserved. However, the photoreceptors in these mice degenerated, and the rate of the cell loss increased with the level of the transgene expression, unlike in transgenic mice that overexpressed normal GCAP1. These results provide the first direct evidence that a mutation linked to congenital blindness increases Ca^{2+} in the outer segment, which may trigger the apoptotic process.

Key words: **retina; guanylyl cyclase; calcium; retinal dystrophy; transgenic mice; cone; retinal degeneration; photoreceptors**

Introduction

Guanylyl cyclase-activating proteins (GCAPs) are EF-hand calcium-binding proteins that activate photoreceptor guanylyl cyclase when free Ca^{2+} concentrations in rods and cones fall after illumination and inhibit the cyclase when free Ca^{2+} reaches its resting level in the dark (for review, see Palczewski et al., 2000; Olshevskaya et al., 2002). The absorption of light in rod and cone outer segments activates the photopigment, triggering an increase in the activity of a cGMP phosphodiesterase (PDE), the enzyme that hydrolyzes cGMP, leading to the closure of cGMP-gated channels in the outer segment. Photoreceptor membrane guanylyl cyclase (retGC1/2 or GC-E/F) (Garbers and Lowe, 1994; Garbers, 1999), regulated by GCAPs, subsequently restores the level of cGMP. Closure of the cGMP-gated channels in the light produces a decrease in outer segment Ca^{2+} concentration (Gray-Keller and Detwiler, 1994; Sampath et al., 1998, 1999; Woodruff et al., 2002), causing Ca^{2+} to dissociate from the GCAPs, and that stimulates retGC to synthesize more cGMP and to reopen the cGMP-gated cation channels. This GCAP-dependent activation of the cyclase plays an important role both in shaping the photoreceptor light response and in light adaptation (Fain et al., 2001; Mendez et al., 2001; Burns et al., 2002).

Several forms of congenital blindness in humans associate with mutations in the *GUCA1A* gene, which encodes GCAP1 (Payne et al., 1998; Wilkie et al., 2001). One of them, causing a substitution Y99C, has been linked to a late-onset congenital dominant cone dystrophy; *in vitro* studies of recombinant GCAP1 have shown that this mutation reduces its Ca^{2+} sensitivity (Dizhoor et al., 1998; Sokal et al., 1998; Wilkie et al., 2001). These results gave rise to the following hypothesis about the functional role of the Y99C GCAP1 in photoreceptor death. In normal rods and cones the Ca^{2+}-binding sites of GCAP1 are occupied fully in the dark, and the cyclase is mainly inactive. However, in the presence of the mutant GCAP1, which has lower affinity for Ca^{2+}, guanylyl cyclase remains partially active at normal high Ca^{2+} levels in the dark; hence, free cGMP concentration increases. As a result, a higher than normal percentage of cGMP-gated channels will be open, thus letting excess Na^{+} and Ca^{2+} enter the outer segment (Dizhoor et al., 1998; Fain and Lisman,

Received March 15, 2004; revised May 24, 2004; accepted May 25, 2004.

This work was supported by National Institutes of Health Grants EY11522 (A.M.D.), EY12944 (C.L.M.), EY01844 (G.L.F.), and Center Grant P30 ES06639 (Y.S.H.). We thank Alexander Ermilov and Ronald Barrett for excellent technical assistance, Arkady Lyubarsky for building the ERG setup, and James Hurley for stimulating discussions.

*E.V.O., P.D.C., and M.L.W. contributed equally to this work.

Correspondence should be addressed to A. M. Dizhoor, Pennsylvania College of Optometry, 8360 Old York Road, Elkins Park, PA 19027. E-mail: adizhoor@pco.edu.

DOI:10.1523/JNEUROSCI.0963-04.2004

 0270-6474/04/246078-08$15.00/0

1999; Dizhoor, 2000; Palczewski et al., 2000; Olshevskaya et al., 2002).

To test this hypothesis, we produced transgenic mice that express Y99C GCAP1. We show that this mutation alters the Ca^{2+} sensitivity of cyclase regulation in photoreceptors of these animals such that cyclase remains active at the normal dark level of outer segment Ca^{2+}. The light responses of Y99C GCAP1 rods are affected only slightly, but both rods and cones degenerate at a rate consistent with the amount of expression of the mutant protein. Direct measurement of the intracellular free Ca^{2+} in the rods reveals an abnormal increase in Ca^{2+} that correlates with Y99C GCAP1 expression. These experiments provide the first direct evidence for a role of high Ca^{2+} in congenital retinal dystrophy.

Materials and Methods

The Y99C GCAP1 transgenic mice. All experimental procedures with the mice in this study were conducted in accordance with National Institutes of Health guidelines, as approved by the institutional animal investigation committees. We used a 4.2 kbp fragment of the mouse opsin gene as a promoter-containing region active in both rods and cones (Woodford et al., 1994) inserted between the *Kpn*I and *Xho*I sites of pBluescript (Stratagene, La Jolla, CA). We amplified a short fragment containing the opsin translation initiation signal by PCR, added an *Nco*I site, replaced the ATG codon with 0.6 kbp of the bovine Y99C GCAP1 cDNA *Nco*I/*Bam*HI fragment excised from pET11 vector (Dizhoor et al., 1998; Krylov et al., 1999), and inserted the joint fragment into the *Xho*I/*Bam*HI sites. The construct also contained a 0.5 kbp modified fragment of mouse protamine 1 gene as a polyadenylation signal (Raport et al., 1994) inserted into *Bam*HI/*Xba*I sites. After the final construct was sequenced, it was excised by *Kpn*I/*Xba*I digestion, gel-purified, and injected into male pronuclei of fertilized B6/D2 hybrid mouse eggs, which then were implanted into pseudo-pregnant females. Tail DNA from the progeny was screened by PCR and DNA blot, and then the transgene-positive mice were mated with C57B6 mice (Taconic, Germantown, NY). We found no *PDE6b*^{rd1}, *Prph2*^{rd2}, or *Nr2e3*^{rd7} mutations (Pittler and Baehr, 1991; Ma et al., 1995; Akhmedov et al., 2000; Chang et al., 2002) in the resultant mouse lines. To detect transgenic GCAP1 expression by immunoblot, we homogenized retinas from 3- to 4-week-old mice in a Laemmli SDS sample buffer containing 4 mM EGTA. After electrophoresis in 15% polyacrylamide gel, the retinal proteins were transferred onto Immobilon-P membrane (Millipore, Bedford, MA), probed with affinity-purified rabbit anti-GCAP1 antibody raised against purified recombinant GCAP1, and visualized by using a Femto Supersignal kit (Pierce, Rockford, IL). To compare phototransduction proteins expression, we homogenized each sample containing three retinas in Laemmli SDS sample buffer; 10 μl aliquots were subjected to electrophoresis in 7.5 or 15% polyacrylamide gel and immunoblot. The blot was probed with antibodies against rhodopsin (Abcam, Cambridge, MA), Gαt1, Gβ1 (Santa Cruz Biotechnology, Santa Cruz, CA), CNG1 (a gift from Dr. R. Molday, University of British Columbia), PDE6α, and PDE6β (Abcam) and visualized as described above. The samples for rhodopsin detection were not boiled before electrophoresis.

Recombinant GCAP1 and anti-GCAP1 antibody. GCAP1 cDNA cloned from mouse and bovine retinal cDNA libraries was expressed from a pET11d vector in a BLR(DE3)pLysS *Escherichia coli* strain, and the protein was fast protein liquid chromatography-purified (FPLC-purified) to >90% as described (Dizhoor et al., 1998; Krylov et al., 1999). We used the purified GCAP1 as antigen to produce rabbit polyclonal antibodies and as immunosorbent to affinity-purify the anti-GCAP1 antibody.

Electroretinography. We followed the electroretinogram (ERG) protocol of Lyubarsky et al. (2002), using an SWE BMA-200 AC/DC Bioamplifier and a Tektronix 2205 20 MHz oscilloscope (Beaverton, OR). The signal output was recorded with Axotape 2 software. Mice were dark-adapted for 8–12 hr and then sedated under dim red light (20 mg/kg ketamine and 8 mg/kg xylazine). Tropicamide eye drops (0.5%) were applied to the corneas to dilate the pupils, and the mice were dark-adapted again for at least 10 min before the ERG recording. During the whole procedure the mice were maintained at 37°C on a heated plate. The corneal electrode consisted of a platinum wire in a small concave transparent plastic holder filled with a drop of water. A 1 msec flash adjusted by a 540 nm interference filter and neutral density filters delivered light through the window of an aluminum foil-lined ERG recording chamber, with intensities ranging from 0.72 to 23,900 photons/μm^{-2} at the cornea. An unfiltered saturating white flash was used to evoke the maximal a-wave amplitude with 4 min intervals between flashes. S cone-driven b-waves were recorded by using 360 nm test flashes of 980, 1700, and 3240 photons/μm^{-2} at the cornea, superimposed on a constant incandescent light background of 36.5 scotopic lux.

Histology and immunocytochemistry. Mice were killed by lethal injection of ketamine/xylazine and cervical dislocation and perfused through the heart, first with DMEM–PBS and then with 1% glutaraldehyde in 0.1 M Sorensen phosphate buffer solution, pH 7.2. The eyes were removed and fixed for 3 hr more in 0.8% glutaraldehyde/2% OsO_4/0.1 M Sorensen phosphate buffer solution on ice, washed briefly with PBS, and then dehydrated by using ethanol solutions and propyleneoxide; they were embedded in Embed resin (Electron Microscopy Sciences, Fort Washington, PA), cut into 1-μm-thick sections, and stained with a methylene blue/azure mixture for bright-field microscopy. For immunocytochemistry the eyes were fixed in 4% paraformaldehyde, pH 7.2, for 6–8 hr, embedded in OCT medium, and frozen. The 10-μm-thick sections were taken with a Bright OFT 5000 cryostat. The cryosections were incubated in blocking solution (1% goat serum, 1% bovine serum albumin, 0.05% Triton X-100 in TBS buffer, pH 7.5) for 1 hr; then primary antibodies diluted in TBS containing 0.3% Triton X-100 were applied overnight at 4°C. After being washed twice with TBS for 15 min at room temperature, the sections were incubated with secondary fluorescent antibodies for 1 hr at room temperature under dim dark-orange light, washed twice more with TBS, covered with DAPI-containing Vectashield mounting medium (Vector Laboratories, Burlingame, CA), and photographed with an Olympus BX51 microscope equipped with a Magnafire imaging system. We used FITC-peanut agglutinin (Sigma Aldrich, St. Louis, MO) to label cone sheaths, rabbit polyclonal affinity-purified anti-GCAP1 antibody (as above), rabbit polyclonal Gαt1 (Santa Cruz Biotechnology) anti-transducin antibody to label rod outer segments, and mouse monoclonal anti-Gα0 antibody (Santa Cruz Biotechnology) to counterstain the inner retina (Haverkamp and Wassle, 2000). Fluorescent secondary antibodies were AlexaFluor 568-conjugated goat anti-mouse IgG or goat anti-rabbit IgG (Molecular Probes, Eugene, OR) and FITC-labeled goat anti-rabbit IgG (Cappel/ICN, West Chester, PA/Aurora, OH).

RetGC activity. Dark-adapted mouse retinas aged 3–4 weeks or 6 months were frozen in liquid nitrogen, thawed, and homogenized under infrared illumination on ice in 1.5 ml test tubes with a motor-driven plastic cone-shaped pestle in 250 μl of (in mM) 120 KCl, 60 MOPS, pH 7.2, 10 NaCl, 4.6 $MgCl_2$, 0.2 ATP, plus 50 μM zaprinast, 50 μM dipyridamole, 20 μg/ml leupeptin, 20 μg/ml aprotinin. Each 25 μl of retGC assay reaction [modified from Olshevskaya et al. (1997) and Hurley and Dizhoor (2000), as described by Peshenko and Dizhoor (2004)] contained 1 mM GTP, ~1 μCi [α-^{32}P]GTP, 0.1 μCi [8-^{3}H] cGMP (PerkinElmer Life Sciences, Emeryville, CA), and (in mM) 4 cGMP, 0.3 ATP, 2.3 $MgCl_2$, 30 MOPS, pH 7.2, 5 NaCl, 60 KCl, plus 25 μM each Zaprinast and dipyridamole, 4 μg/ml each leupeptin and aprotinin, and 2 mM Ca^{2+}/EGTA buffers prepared as described (Tsien and Pozzan, 1989; Marks and Maxfield, 1991; Brooks and Storey, 1992). We started the reaction by adding retinal homogenate and performed it at 30°C for 12 min under infrared illumination. The reaction was stopped by heating at 95°C for 2 min; the products of the reaction were analyzed by thin-layer chromatography as described (Koch and Stryer, 1988; Hurley and Dizhoor, 2000).

Calcium determinations in rods. We killed the animals, removed the eyes, and chopped the retina into small pieces as previously described (Woodruff et al., 2002, 2003). We pipetted the pieces into an open perfusion chamber on the stage of an inverted microscope (Zeiss Axiovert 135TV, Oberkochen, Germany) and exposed them for 30 min at room temperature to 10 μM fluo-5F AM (Molecular Probes/Invitrogen, San Diego, CA). We then perfused the pieces at 37°C with bicarbonate-

buffered DMEM [D-2902, Sigma; supplemented with (in mM): 15 $NaHCO_3$, 2 Na-succinate, 0.5 Na-glutamate, 2 Na-gluconate, and 5 NaCl]. We illuminated rods with 488 nm light from an argon gas laser (American Laser), focused as a 10-μm-diameter spot on the outer segment. To minimize dye bleaching, we attenuated the intensity of the laser to 2–5 $\times$ 10^{10} photons per μm^{-2}/sec with reflective neutral density filters. We detected emission with a low dark-count photomultiplier tube (PMT) with a restricted photocathode (model 9130/100A; Electron Tubes, Rockaway, NJ) for which the current was amplified by a low-noise current-to-voltage converter (PDA-700; TeraHertz Technology, Oriskany, NY). The signal was filtered by a low-pass eight-pole Bessel filter (Frequency Devices, Haverhill, MA) and stored for analysis on a PC. We recorded the temperature of the perfusate within 0.5 mm of the rod with a miniature thermocouple and a digital thermometer to determine the binding constant of the dye (Woodruff et al., 2002). We calibrated the intracellular concentration of Ca^{2+} in darkness and after illumination by using the following equation: $[Ca^{2+}] = K_D(F - F_{min})/(F_{max} - F)$, where K_D is the temperature-adjusted dissociation constant of the dye–Ca^{2+} binding, F is the measured fluorescence at the beginning of the recording or at steady state, and F_{min} and F_{max} are the fluorescence minimum (at low Ca^{2+}) and fluorescence maximum (at high Ca^{2+}). We determined F_{min} by exposing the rod first to zero Ca^{2+} solution containing a 10 μM concentration of the Ca^{2+} ionophore ionomycin plus (in mM): 140 NaCl, 3.6 KCl, 3.08 $MgCl_2$, 2.0 EGTA, and 3.0 HEPES, pH 7.4. We then determined F_{max} by exposing the rod to high Ca^{2+} solution containing (in mM): 50 $CaCl_2$, 3.6 KCl, 3.0 HEPES, 140 sucrose, pH 7.4.

Single-cell suction electrode recording. Nontransgenic, Y99C L52H, and Y99C L53 mice aged 3–12 weeks were dark-adapted overnight, and all subsequent preparation of tissue was performed under infrared illumination. Animals were anesthetized with CO_2 and killed by cervical dislocation. Retinas were isolated into oxygenated Leibovitz's L-15 medium and stored on ice until used, whereon a small piece of retina was chopped finely in L-15 containing DNase I, type IV (Sigma) and loaded into a recording chamber. The tissue was perfused with Ringer's solution containing (in mM): 144 Na^+, 3.6 K^+, 1.2 Ca^{2+}, 2.4 Mg^{2+}, 123.3 Cl^-, 10 HEPES, 20 HCO_3^-, 0.02 EDTA, 10 glucose, 0.5 glutamate, 3 succinate, BME vitamins, and MEM amino acids, pH 7.4, equilibrated with 95% O_2/5% CO_2, and heated to 36–38°C. The outer segment of a rod was drawn into a silanized glass suction pipette that contained identical medium except that HCO_3^- was replaced with Cl^-, and vitamins and amino acids were omitted. The current flowing across the outer segment membrane was recorded with a current-to-voltage converter (Axopatch 200A; Axon Instruments, Foster City, CA), low-pass filtered at 30 Hz (–3 dB, eight-pole Bessel; Frequency Devices), and digitized at 400 Hz. No correction was made for the 16.9 msec delay introduced by low-pass filtering. Some records additionally were filtered digitally at 14 Hz by convolution with a Gaussian (IgorPro software; WaveMetrics, Lake Oswego, OR). Rods were stimulated with 20 msec pulses of light from a xenon-arc source that was bandpass-filtered at 500 nm (10 nm bandwidth at half-maximal transmission; Omega Optical, Brattleboro, VT).

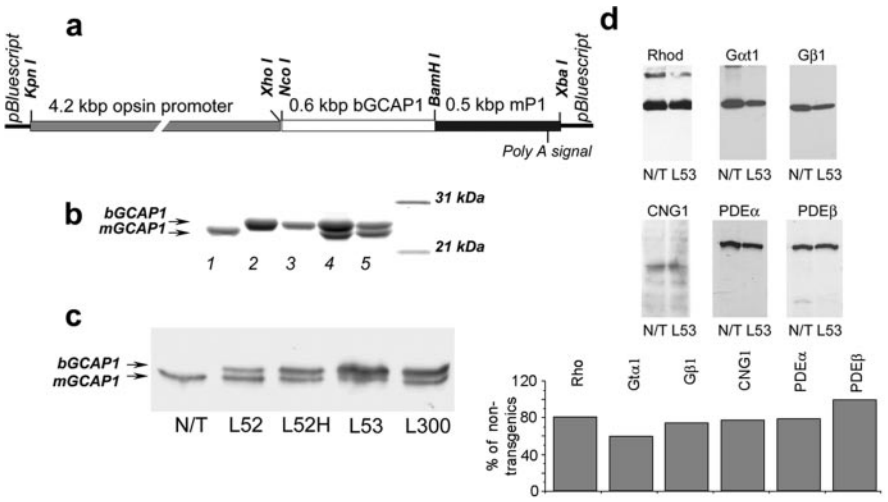

Figure 1. Expression of the exogenous GCAP1 in transgenic mice. *a*, DNA construct for the Y99C GCAP1 expressed in transgenic mice (for details, see Materials and Methods). *b*, Electrophoretic mobility of purified mouse and bovine GCAP1. Shown is a Coomassie-stained SDS-PAGE gel loaded with the following: lane 1, 2 μg of mouse GCAP1 (mGCAP1); lane 2, 5 μg of bovine GCAP1 (bGCAP1); lane 3, 2 μg of Y99C bGCAP1; lane 4, mGCAP1 plus bGCAP1; lane 5, mGCAP1 plus Y99C bGCAP1. *c*, Expression of the transgene in some of the transgenic mouse lines (nontransgenic mouse Y99C bGCAP1 in lines L52, L52H, and L53 and normal bGCAP1 expression in line L300) detected by immunoblot. The bottom band corresponds to the endogenous mGCAP1, and the top band is a product of the bovine transgene. *d*, Expression of other phototransduction proteins in nontransgenic siblings and L53 mice. Retinas from 3-week-old mice were analyzed by SDS electrophoresis and probed with antibodies against rhodopsin, Gαt1, Gβ1, CNG1, PDE6α, and PDE6β as described in Materials and Methods. The corresponding signal intensities in the L53 mice are plotted in the bottom panel as a percentage of the nontransgenic control.

Results

Expression of Y99C GCAP1 in mouse retinas

The Y99C GCAP1-linked retinal dystrophy has a dominant phenotype in human patients (Payne et al., 1998). Although normal GCAP1 and GCAP2 compete with Y99C GCAP1, they cannot maintain normal Ca^{2+} sensitivity of cyclase regulation in the presence of the mutant GCAP1 *in vitro* (Dizhoor et al., 1998; Sokal et al., 1998), consistent with the dominant phenotype of the retinal dystrophy. We therefore expressed Y99C GCAP1 on a background of normal mouse GCAP1 under control of a 4.2 kbp 5′ opsin gene fragment containing a promoter region active in both rods and cones (Woodford et al., 1994). To distinguish between the endogenous mouse protein and the product of the transgene, we used a bovine GCAP1 cDNA sequence (Fig. 1*a*). Unlike human GCAP1, the bovine homolog has a sufficiently lower electrophoretic mobility when compared with the mouse GCAP1 so that it can be distinguished reliably on an SDS gel (Fig. 1*b*). The regulatory properties of bovine Y99C GCAP1 *in vitro* are similar to those of human Y99C GCAP1 (Dizhoor et al., 1998; Sokal et al., 1998).

We obtained various levels of Y99C GCAP1 expression in mouse lines produced independently from different founders. One of them (L52, Y99C+/–) produced Y99C GCAP1 at a ratio of 0.5–0.7:1 relative to endogenous GCAP1 and at a ratio of 1–2:1 in the homozygous state (L52H, Y99C+/+), as determined by immunoblot (Fig. 1*c*). A second line (L53, Y99C+/–) had a higher level of expression (3–4:1). For comparison, we also generated a line (L300) that expressed *normal* bovine GCAP1 at this same high level. Four other lines (L36, L39, L128, and L52X) expressed Y99C at a level exceeding that in L300 by several-fold (data not shown).

Morphological changes in mouse retinas caused by the expression of Y99C GCAP1

Although early development of the retina appeared to be normal in mice expressing Y99C GCAP1, striking changes occurred as the photoreceptors started to extend outer segments. All Y99C mice had shorter rod outer segments, a difference that was detectable as early as 3 weeks of age, also resulting in a small, nearly proportional, decrease in rhodopsin, CNG1, Gα1, Gβ1, PDE6α, and PDE6β content in degenerating retinas at that age (Fig. 1*d*).

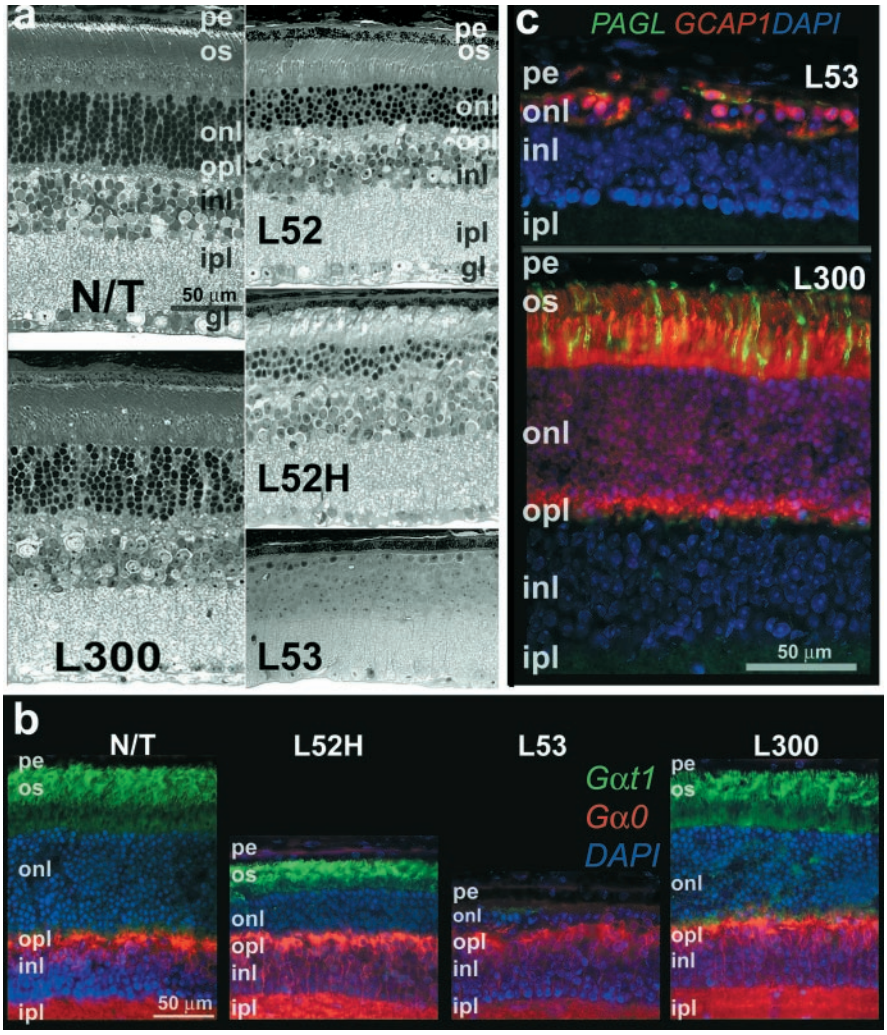

Figure 2. Histological changes in the retinas of 6-month-old mice caused by Y99C GCAP1 expression. *a*, Light microscopy of retinal sections from a nontransgenic mouse (N/T), Y99C GCAP1 mice (L52, L52H, and L53), and a mouse that overexpressed normal GCAP1 (L300). The outer nuclear layer, which consists almost entirely of rod nuclei, becomes markedly thinner as the rods degenerate. Pe, Retinal pigment epithelium; os, photoreceptor outer segments; onl, outer nuclear layer; opl, outer plexiform layer; inl, inner nuclear layer; ipl, inner plexiform layer; gl, ganglion cell layer. *b*, Immunofluorescence of photoreceptor-specific and inner retina-specific markers in cryosections of mouse retinas. Green fluorescence, FITC anti-rod α-transducin (Gαt1) as a rod outer segment marker; red fluorescence, mouse anti-Gα0 as an inner retina marker; blue fluorescence, nuclei counterstained with DAPI. *c*, L53 Y99C (top) and L300 bGCAP1 (bottom) mouse retinas probed with anti-GCAP1 antibody (red fluorescence) and FITC-peanut agglutinin (green fluorescence) as a marker for cone sheaths. The double labeling of cones produces the yellow color.

By 6 months of age (Fig. 2) many outer segments were gone, but those that remained were still shorter than normal. In addition, photoreceptor nuclei losses were dramatic. The severity of degeneration increased with the level of the Y99C GCAP1 expression. In the strongest expressing lines (L36, L39, L52X, L128), the photoreceptor layer degenerated by one-half in little over 1 month (data not shown). Because of the rapidity and severity of retinal degeneration, these lines were not studied further. The rate of photoreceptor loss was 2–3.5 times slower in L53 and L52H, but the degeneration was progressive, especially in the central and nasal portions of the retina. By 6 months of age only a few photoreceptor nuclei remained in some areas of the L53 retina, and outer segments of both rods and cones were absent (Fig. 2*a–c*). Even in L52, which had the lowest expression of Y99C, outer nuclear layer thickness diminished 30–50% at 6 months. For L52, L52H, and L53 the changes in retinal morphology could not be attributed simply to higher than normal levels of GCAP1, because in the L300 line outer segment length and outer nuclear layer thickness were similar to wild type even at 6 months (Fig. 2*a–c*).

Loss of retinal function in the Y99C mice

Disturbances in the Y99C mouse ERG paralleled the degenerative changes in retinal morphology (Fig. 3*a–c*). The dark-adapted corneal negative a-wave, caused primarily by the shut-off of dark current in rods, was reduced at 5–7 months of age in L52H Y99C transgenic mice to 83 ± 6 μV (mean ± SEM; $n = 6$) and was absent in L53 ($n = 7$) (Fig. 3*a,b*). The a-wave amplitude in nontransgenic siblings was 388 ± 48 μV ($n = 8$). Despite the high level of normal bovine GCAP1 expression in L300 mice, their retinas retained a full complement of photoreceptors, with outer segments of normal length (Fig. 2), so there was no significant change in maximal a-wave amplitude (402 ± 29 μV; $n = 6$) (Fig. 3*a,b*). Although the a-wave could not be measured in L53 at 6 months, sometimes there were enough surviving photoreceptors to give rise to a small corneal positive b-wave, driven primarily by the excitation of the ON-bipolar cells. Photoreceptor loss was not restricted to rods; the cone-driven b-wave in 6-month-old Y99C L53 mice also was suppressed when compared with the nontransgenic littermates (Fig. 3*c*). The cone-driven b-wave in L300 was normal.

RetGC activity in Y99C GCAP1 mouse retinas

To learn how transgene expression affected retGC activity, we determined guanylyl cyclase activity in retinal homogenates as a function of Ca^{2+}. In older Y99C animals lacking photoreceptors but retaining inner retinal neurons in abundance, Ca^{2+}-sensitive guanylyl cyclase activity was undetectable (Fig. 4, inset). Therefore, essentially all retGC activity in the retina originated from the photoreceptors. Retinal homogenates of young Y99C mice exhibited prominent shifts in cyclase sensitivity to higher Ca^{2+} ranges (Fig. 4). The higher proportion of the Y99C to native GCAP1 in L53 than in L52H resulted in a larger shift in $K_{m,Ca}$ (4.3-fold for L53 compared with 2.6-fold for L52H). These results are in good agreement with previous work that used recombinant Y99C (Dizhoor et al., 1998). It is of some interest that overexpressed normal GCAP1 also caused a lesser, yet noticeable shift in the guanylyl cyclase Ca^{2+} sensitivity in L300, likely because GCAP1 alone inhibits retGC at higher $K_{m,Ca}$ than GCAP1 and GCAP2 acting together (Hwang et al., 2003). The shifts in Ca^{2+} sensitivity of guanylyl cyclase activity in Y99C mice, extending beyond the normal physiological range of 25–250 nM free Ca^{2+} in mouse rods (Woodruff et al., 2002) (Fig. 4, shaded area), predicted that guanylyl cyclase activity would remain partially active in darkness; this can result in elevated free cGMP levels in the dark. Because the free cGMP in resting pho-

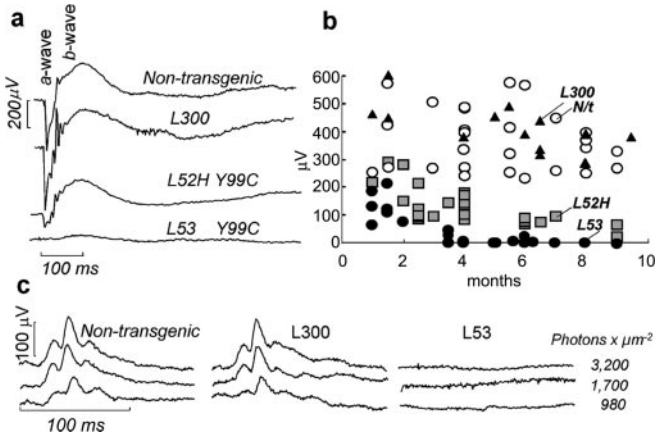

Figure 3. Electroretinographic analysis of mouse retinal function. *a*, Typical responses to a saturating flash in dark-adapted mice at 5–7 months of age; shown are nontransgenic mouse, L300 (normal bCAP1), L52H (Y99C), and L53 (Y99C). *b*, Maximal a-wave amplitudes of dark-adapted mice as a function of age. Open circles, Nontransgenic siblings; filled triangles, L300; shaded squares, L52H; filled circles, L53. Each symbol plots the result obtained from a different mouse. *c*, Typical S cone-driven b-waves recorded from light-adapted mice at 6 months of age in response to incremental 360 nm test flashes.

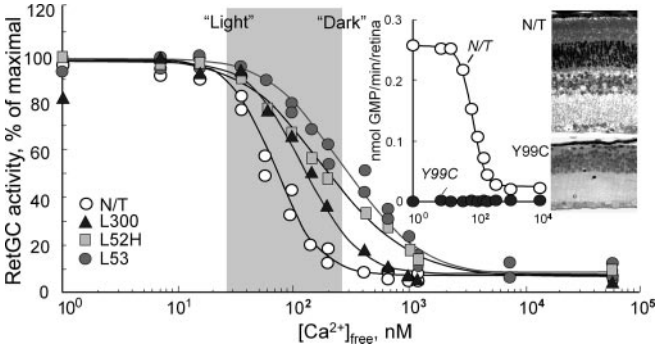

Figure 4. Ca^{2+} sensitivity of retGC in transgenic mouse retinas. Open circles, Nontransgenic siblings; filled triangles, L300; shaded squares, L52H; shaded circles, L53. Lines are fittings with the following function: $A = (A_{max} - A_{min})/[1 + ([Ca]_{free}/K_{m,Ca})^n] + A_{min}$, where A is retGC activity and n is the Hill coefficient. $K_{m,Ca}$ was 70 nM (N/T), 150 nM (L300), 180 nM (L52H), and 300 nM (L53); $n = 2.2$ (N/T), 1.6 (L300), 1.1 (L52H), and 1.2 (L53). The shaded area represents the normal range of free Ca^{2+} change in mouse rods between light and dark (Woodruff et al., 2002). Inset, All detectable Ca^{2+}-sensitive retGC activity in the retina belongs to photoreceptors. Retinas were collected from Y99C L128 mice and their nontransgenic siblings after 6 months of age (the corresponding retinal histology is shown on the right). Open circles, Nontransgenic siblings; filled circles, Y99C mice. Mouse retinas that lack photoreceptors also lack the retGC activity.

toreceptors (3–4 μM) (Pugh et al., 1997) is <5% of the total cGMP, most of which is bound to the noncatalytic sites on PDE6 (Gillespie and Beavo, 1989), it cannot be measured directly in the retina by using biochemical assays (Kilbride and Ebrey, 1979; Govardovskii and Berman, 1981). Still, free cGMP regulates the Na^+/Ca^{2+} channels in the outer segment with high cooperativity; therefore, changes in free cGMP can affect the channel activity significantly. Below we determined the physiological impact of this perturbation on free Ca^{2+} level and photoresponses in single rods.

Elevated Ca^{2+} concentration in dark-adapted Y99C photoreceptors

Higher than normal rates of cGMP synthesis would enhance the opening of cGMP-gated channels in Y99C rods and permit a greater influx of Ca^{2+} into the outer segment. We tested this

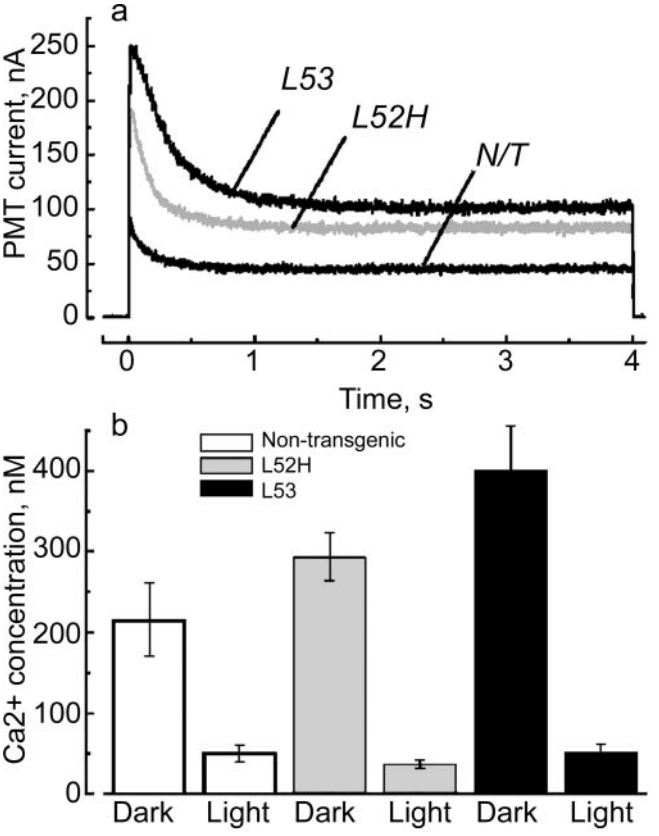

Figure 5. Free Ca^{2+} concentration. *a*, Fluorescence of fluo-5F-filled rods excited by the laser for 4 sec. Traces are the means of five rods for nontransgenic, L52H, and L53. *b*, Ca^{2+} concentrations after calibration of absolute fluorescence (see Materials and Methods). Error bars indicate the mean ± SEM for 10 rods each from L52H and L53 and eight rods from nontransgenic littermates.

prediction by comparing the Ca^{2+} in L53 and L52H rod outer segments with that of nontransgenic littermates. Rods were filled with the fluorescent dye fluo-5F and illuminated with a laser (see Materials and Methods). The initial fluorescence at the beginning of the measurement (Fig. 5*a*) was proportional to the dark-adapted Ca^{2+} concentration and was higher for L53 and L52H rods than for nontransgenic rods. Closure of the cGMP-gated channels in response to the measuring light and subsequent removal of Ca^{2+} by Na^+/Ca^{2+}–K^+ exchange brought about a decline in fluorescence over time. The initial fall in Ca^{2+} was slower for Y99C animals than for nontransgenics, probably because there was a higher concentration of Na^+ in the Y99C outer segments that slowed the rate of Na^+-dependent Ca^{2+} removal. The fluorescence decrease also occurred after a slight delay in the Y99C rods, with a longer delay in the faster-degenerating L53 line than in L52H. Furthermore, the final Ca^{2+} concentration was reached after a few seconds in nontransgenic rods (Fig. 5*a*) but only after 30–60 sec in the Y99C rods (data not shown).

Because the initial fluorescence was larger in Figure 5*a* for the rods from L52H and L53 animals than from nontransgenic mice, it seemed likely that the dark steady-state Ca^{2+} concentration in the transgenic animals was elevated. To investigate this possibility more quantitatively, we performed an *in situ* calibration of the Ca^{2+} concentration, as described in Materials and Methods. For each of 10 rods from L52H and L53 animals and for eight rods from nontransgenic littermates, we individually exposed the rods successively to a zero Ca^{2+} solution and a high Ca^{2+} solution in the presence of ionomycin to determine for each rod the value of

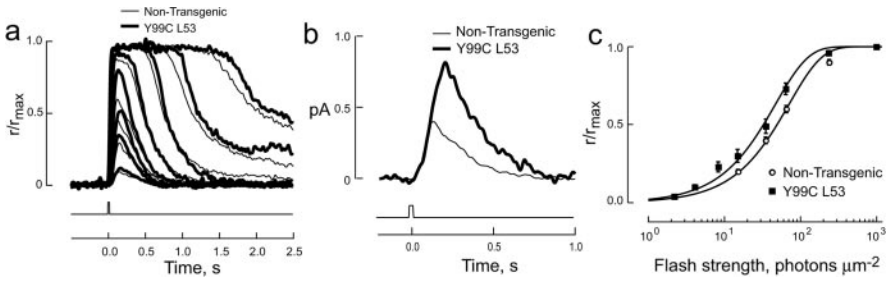

Figure 6. Flash response kinetics and sensitivity in Y99C GCAP1 rods. *a*, Averaged responses recorded from a nontransgenic rod and a rod expressing Y99C GCAP1 (line L53) to flashes of 4, 14.5, 35, 62, 227, 968, 3520, and 15,800 photons/μm^{-2}. Flash monitor is the lowest trace. *b*, Larger, slower single photon responses in L53 rods. The single photon response of an individual rod was taken as its dim flash response scaled to the ratio of the ensemble variance to the mean amplitude for that rod (cf. Baylor et al., 1979b). The average single photon response from L53 rods (thick trace, $n = 11$) was 1.8-fold larger and peaked 54 msec later than that of nontransgenic rods (thin trace, $n = 17$). The integration times, given as the integrals of the responses divided by their amplitudes, were 317 and 230 msec for L53 and nontransgenic rods, respectively. *c*, Averaged peak response amplitudes normalized to the maximal response amplitude (r/r_{max}) of nontransgenic ($n = 17$) and Y99C L53 ($n = 11$) rods as a function of flash strength. Lines are fittings with a saturating exponential function, $r/r_{max} = 1-e^{-ki}$, where i is the flash strength, $k = ln(2)/i_0$, and i_0 is the flash strength giving rise to the half-maximal response. i_0 was 52 ± 3 photons/μm^{-2} for nontransgenic rods and 39 ± 6 photons/μm^{-2} for Y99C L53 (mean ± SEM). Error bars indicate SEM.

the minimum fluorescence F_{min} and the maximum fluorescence F_{max}. These numbers, together with a previously determined value for the K_D for fluo-5F (Woodruff et al., 2002), were used to calculate the free Ca^{2+} concentration. This procedure corrects for any differences in dye loading among the rods or for possible differences in laser intensity from one experiment to another.

The results of these experiments (Fig. 5*b*) give a mean free Ca^{2+} in dark-adapted nontransgenic rods of 220 nM, consistent with previous determinations (Woodruff et al., 2002, 2003), but a concentration 1.4-fold higher in L52H and 1.9-fold higher in L53 rods in darkness. No differences in the Ca^{2+} concentration were detected in bright light after closure of all of the cGMP-gated channels. Thus by opening more cGMP-gated channels per unit length of outer segment in darkness, Y99C forced rods to operate over a wider range of Ca^{2+} concentrations.

Suction electrode recording of individual rods

Modulation of retGC by Ca^{2+} plays an important role in the signaling of light by photoreceptors (for review, see Fain et al., 2001). Constitutively active guanylyl cyclase might be expected to increase maximal response amplitude and flash sensitivity because of an increase in free cGMP. In addition, the recovery of the photoresponse might be prolonged because of loss of Ca^{2+}-regulated feedback. In suction electrode recordings the expression of Y99C had surprisingly little effect on the photoresponses of L52H (data not shown) and L53 rods over a wide range of flash strength (Fig. 6*a*). Therefore, guanylyl cyclase activity did not remain constant at the fully activated level during the course of the response. Instead, guanylyl cyclase must have been subjected to Ca^{2+}-dependent regulation, although the slight prolongation of the response suggests that regulation operated over a restricted dynamic range and/or had a delayed onset. The amplitude and the time-to-peak of the single photon response were larger for the L53 rods (Fig. 6*b*), providing evidence that free cGMP was higher than normal. The flash giving rise to a half-maximal response (i_0) was reduced to a slightly lesser extent than expected from the enlarged quantal response (Fig. 6*c*), primarily because L53 rod outer segments were shorter, so their ability to capture photons was reduced. Because the rod cGMP-gated channel is outwardly rectifying (Baylor and Nunn, 1986), the current circulating in darkness is proportional to rod outer segment length (cf. Baylor et al., 1979a). Therefore, shortening of the outer segments also may have explained our failure to observe an increase in maximal response amplitude: 5.7 ± 0.8 pA (L53, $n = 12$) versus 6.2 ± 0.6 pA (N/T, $n = 17$).

Discussion

Our experiments demonstrate that the Y99C GCAP1 mutation, which has been shown to be associated with photoreceptor dystrophy in humans, also produced photoreceptor degeneration in mouse, and the rate of degeneration correlated with the level of expression of the mutant transgene. Transgenic retinas showed abnormal regulation of retGC much like that previously described for purified Y99C GCAP1 *in vitro* such that the cyclase remained partially activated at the normal dark Ca^{2+} concentration of the rod (Fig. 4). We infer that higher than normal cyclase activity in the dark increased opening of the cGMP-gated channels, producing an increase in the free Ca^{2+} concentration (Fig. 5), which was greater in the faster-degenerating L53 line than in the L52H line.

Remarkably, the light responses of the rods in animals expressing the Y99C transgene were nearly normal (Fig. 6). In particular, the maximum value of the photoresponse and therefore of the circulating (dark) current was not increased greatly in L53 rods as compared with nontransgenic rods, although the Ca^{2+} was greater. The likely explanation for this seeming contradiction was that the outer segments of the Y99C rods were significantly shorter. Thus the enhanced dark current (including Ca^{2+} influx) sustained per unit outer segment length in the Y99C rods elevated intracellular Ca^{2+} but did not alter the maximum value of the photocurrent. Because the dynamic range of modulation of the cyclase was shifted toward higher free Ca^{2+} in rods expressing Y99C GCAP1, there was no dramatic change in flash response kinetics or sensitivity. This may explain why patients who inherit the Y99C mutation do not develop symptoms of visual loss immediately after birth but only at mid-life, concomitant with the onset of degeneration in the macula (Payne et al., 1998).

It is unclear why Y99C GCAP1 caused degeneration of both rods and cones in mice, whereas in human patients the same mutation primarily affects cones. This may be a function of the relative levels at which GCAPs 1 and 2 are expressed in rods and cones of different species as well as the relative efficiency of expression of the mutant versus normal *GUCA1A* allele in human rods and cones.

The causal link between Y99C and apoptotic loss of photoreceptors is not yet known. Our study shows that the Y99C mutation raises free cGMP, opens more cGMP-gated channels, and floods the cell with Ca^{2+}. Depolarized membrane potential or higher metabolic load caused by enhanced cGMP turnover and increased Na^+ influx in darkness may contribute to the pathology, but elevated Ca^{2+} probably plays a key role, because an artificial increase in intracellular Ca^{2+} has been shown to activate apoptotic pathways in rods (He et al., 2000). The change in Ca^{2+} concentration is not dramatic but continuous in darkness, and the increase in Ca^{2+} correlates with the severity of inherited retinal dystrophy. High Ca^{2+} in the outer segment may diffuse to the adjacent mitochondria of the ellipsoid body, triggering apo-

ptosis. Alternatively, Y99C may stimulate retGC present in the inner segment (Dizhoor et al., 1994; Liu et al., 1994; Olshevskaya et al., 2002) and open cGMP-gated channels located there (Watanabe and Matthews, 1988). In addition to GCAP1, it is likely that mutations in certain other genes linked to retinal dystrophy in human patients, e.g., *retGC1* (Kelsell et al., 1998; Tucker et al., 1999; Wilkie et al., 2000; Ramamurthy et al., 2001) or *PDE6b* (McLaughlin et al., 1995), or in animal models (for review, see Petersen-Jones, 1998; Chang et al., 2002) also produce photoreceptor degeneration via an increase in Ca^{2+}. Some other forms of photoreceptor degeneration recently have been associated with a *decrease* in Ca^{2+} (Woodruff et al., 2003). It therefore appears that free Ca^{2+} in the outer segment is critically important to the survival of the cell and must be regulated within a narrow range to prevent apoptosis (Lem and Fain, 2004).

References

Akhmedov NB, Piriev NI, Chang B, Rapoport AL, Hawes NL, Nishina PM, Nusinowitz S, Heckenlively JR, Roderick TH, Kozak CA, Danciger M, Davisson MT, Farber DB (2000) A deletion in a photoreceptor-specific nuclear receptor mRNA causes retinal degeneration in the *rd7* mouse. Proc Natl Acad Sci USA 97:5551–5556.

Baylor DA, Nunn BJ (1986) Electrical properties of the light-sensitive conductance of rods of the salamander *Ambystoma tigrinum*. J Physiol (Lond) 371:115–145.

Baylor DA, Lamb TD, Yau K-W (1979a) The membrane current of single rod outer segments. J Physiol (Lond) 288:589–611.

Baylor DA, Lamb TD, Yau K-W (1979b) Responses of retinal rods to single photons. J Physiol (Lond) 288:613–634.

Brooks SP, Storey KB (1992) Bound and determined: a computer program for making buffers of defined ion concentrations. Anal Biochem 201:119–126.

Burns ME, Mendez A, Chen J, Baylor DA (2002) Dynamics of cyclic GMP synthesis in retinal rods. Neuron 36:81–91.

Chang B, Hawes NL, Hurd RE, Davisson MT, Nusinowitz S, Heckenlively JR (2002) Retinal degeneration mutants in the mouse. Vision Res 42:517–526.

Dizhoor AM (2000) Regulation of cGMP synthesis in photoreceptors: role in signal transduction and congenital diseases of the retina. Cell Signal 12:711–719.

Dizhoor AM, Lowe DG, Olshevskaya EV, Laura RP, Hurley JB (1994) The human photoreceptor membrane guanylyl cyclase, retGC, is present in outer segments and is regulated by calcium and a soluble activator. Neuron 12:1345–1352.

Dizhoor AM, Boikov SG, Olshevskaya EV (1998) Constitutive activation of photoreceptor guanylate cyclase by Y99C mutant of GCAP-1. Possible role in causing human autosomal dominant cone degeneration. J Biol Chem 273:17311–17314.

Fain GL, Lisman JE (1999) Light, Ca^{2+}, and photoreceptor death: new evidence for the equivalent-light hypothesis from arrestin knockout mice. Invest Ophthalmol Vis Sci 40:2770–2772.

Fain GL, Matthews HR, Cornwall MC, Koutalos Y (2001) Adaptation in vertebrate photoreceptors. Physiol Rev 81:117–151.

Garbers DL (1999) The guanylyl cyclase receptors. Methods 19:477–484.

Garbers DL, Lowe DG (1994) Guanylyl cyclase receptors. J Biol Chem 269:30741–30744.

Gillespie PG, Beavo JA (1989) cGMP is tightly bound to bovine retinal rod phosphodiesterase. Proc Natl Acad Sci USA 86:4311–4315.

Govardovskii VI, Berman AL (1981) Light-induced changes of cyclic GMP content in frog retinal rod outer segments measured with rapid freezing and microdissection. Biophys Struct Mech 7:125–130.

Gray-Keller MP, Detwiler PB (1994) The calcium feedback signal in the phototransduction cascade of vertebrate rods. Neuron 13:849–861.

Haverkamp S, Wassle H (2000) Immunocytochemical analysis of the mouse retina. J Comp Neurol 424:1–23.

He L, Poblenz AT, Medrano CJ, Fox DA (2000) Lead and calcium produce rod photoreceptor cell apoptosis by opening the mitochondrial permeability transition pore. J Biol Chem 275:12175–12184.

Hurley JB, Dizhoor AM (2000) Heterologous expression and assays for photoreceptor guanylyl cyclases and guanylyl cyclase activating proteins. Methods Enzymol 315:708–717.

Hwang J-Y, Lange C, Helten A, Hoppner-Heitmann D, Duda T, Sharma RK, Koch K-W (2003) Regulatory modes of rod outer segment membrane guanylate cyclase differ in catalytic efficiency and Ca^{2+} sensitivity. Eur J Biochem 270:3814–3821.

Kelsell RE, Gregory-Evans K, Payne AM, Perrault I, Kaplan J, Yang R-B, Garbers DL, Bird AC, Moore AT, Hunt DM (1998) Mutations in the retinal guanylate cyclase (RETGC-1) gene in dominant cone–rod dystrophy. Hum Mol Genet 7:1179–1184.

Kilbride P, Ebrey TG (1979) Light-initiated changes of cyclic guanosine monophosphate levels in the frog retina measured with quick-freezing techniques. J Gen Physiol 74:415–426.

Koch K-W, Stryer L (1988) Highly cooperative feedback control of retinal rod guanylate cyclase by calcium ions. Nature 334:64–66.

Krylov DM, Niemi GA, Dizhoor AM, Hurley JB (1999) Mapping sites in guanylyl cyclase activating protein-1 required for regulation of photoreceptor membrane guanylyl cyclases. J Biol Chem 274:10833–10839.

Lem J, Fain GL (2004) Constitutive opsin signaling: night blindness or retinal degeneration? Trends Mol Med 10:150–157.

Liu X, Seno K, Nishizawa Y, Hayashi F, Yamazaki A, Matsumoto H, Wakabayashi T, Usukura J (1994) Ultrastructural localization of retinal guanylate cyclase in human and monkey retinas. Exp Eye Res 59:761–768.

Lyubarsky AL, Lem J, Chen J, Falsini B, Iannaccone A, Pugh Jr EN (2002) Functionally rodless mice: transgenic models for the investigation of cone function in retinal disease and therapy. Vision Res 42:401–415.

Ma J, Norton JC, Allen AC, Burns JB, Hasel KW, Burns JL, Sutcliffe JG, Travis GH (1995) Retinal degeneration slow (*rds*) in mouse results from simple insertion of a *t* haplotype-specific element into protein-coding exon II. Genomics 28:212–219.

Marks PW, Maxfield FR (1991) Preparation of solutions with free calcium concentration in the nanomolar range using 1,2-bis(*o*-aminophenoxy) ethane-*N,N,N′,N′*-tetraacetic acid. Anal Biochem 193:61–71.

McLaughlin ME, Ehrhart TL, Berson EL, Dryja TP (1995) Mutation spectrum of the gene encoding the β-subunit of rod phosphodiesterase among patients with autosomal recessive retinitis pigmentosa. Proc Natl Acad Sci USA 92:3249–3253.

Mendez A, Burns ME, Sokal I, Dizhoor AM, Baehr W, Palczewski K, Baylor DA, Chen J (2001) Role of guanylate cyclase-activating proteins (GCAPs) in setting the flash sensitivity of rod photoreceptors. Proc Natl Acad Sci USA 98:9948–9953.

Olshevskaya EV, Hughes RE, Hurley JB, Dizhoor AM (1997) Calcium binding, but not a calcium-myristoyl switch, controls the ability of guanylyl cyclase-activating protein GCAP-2 to regulate photoreceptor guanylyl cyclase. J Biol Chem 272:14327–14333.

Olshevskaya EV, Ermilov AN, Dizhoor AM (2002) Factors that affect regulation of cGMP synthesis in vertebrate photoreceptors and their genetic link to human retinal degeneration. Mol Cell Biochem 230:139–147.

Palczewski K, Polans AS, Baehr W, Ames JB (2000) Ca^{2+}-binding proteins in the retina: structure, function, and the etiology of human visual diseases. BioEssays 22:337–350.

Payne AM, Downes SM, Bessant DAR, Taylor R, Holder GE, Warren MJ, Bird AC, Bhattacharya SS (1998) A mutation in guanylate cyclase activator 1A (GUCA1A) in an autosomal dominant cone dystrophy pedigree mapping to a new locus on chromosome 6p21.1. Hum Mol Genet 7:273–277.

Peshenko IV, Dizhoor AM (2004) Guanylyl cyclase-activating proteins (GCAPs) are Ca^{2+}/Mg^{2+} sensors: implications for photoreceptor guanylyl cyclase (retGC) regulation in mammalian photoreceptors. J Biol Chem 279:16903–16906.

Petersen-Jones SM (1998) Animal models of human retinal dystrophies. Eye 12:566–570.

Pittler SJ, Baehr W (1991) Identification of a nonsense mutation in the rod photoreceptor cGMP phosphodiesterase β-subunit gene of the *rd* mouse. Proc Natl Acad Sci USA 88:8322–8326.

Pugh Jr EN, Duda T, Sitaramayya A, Sharma RK (1997) Photoreceptor guanylate cyclases: a review. Biosci Rep 17:429–473.

Ramamurthy V, Tucker C, Wilkie SE, Daggett V, Hunt DM, Hurley JB (2001) Interactions within the coiled-coil domain of RetGC-1 guanylyl cyclase are optimized for regulation rather than for high affinity. J Biol Chem 276:26218–26229.

Raport CJ, Lem J, Makino C, Chen CK, Fitch CL, Hobson A, Baylor D, Simon MI, Hurley JB (1994) Downregulation of cGMP phosphodiesterase in-

duced by expression of GTPase-deficient cone transducin in mouse rod photoreceptors. Invest Ophthalmol Vis Sci 35:2932–2947.

Sampath AP, Matthews HR, Cornwall MC, Fain GL (1998) Bleached pigment produces a maintained decrease in outer segment Ca^{2+} in salamander rods. J Gen Physiol 111:53–64.

Sampath AP, Matthews HR, Cornwall MC, Bandarchi J, Fain GL (1999) Light-dependent changes in outer segment free-Ca^{2+} concentration in salamander cone photoreceptors. J Gen Physiol 113:267–277.

Sokal I, Li N, Surgucheva I, Warren MJ, Payne AM, Bhattacharya SS, Baehr W, Palczewski K (1998) GCAP1 (Y99C) mutant is constitutively active in autosomal dominant cone dystrophy. Mol Cell 2:129–133.

Tsien R, Pozzan T (1989) Measurement of cytosolic free Ca^{2+} with quin2. Methods Enzymol 172:230–262.

Tucker CL, Woodcock SC, Kelsell RE, Ramamurthy V, Hunt DM, Hurley JB (1999) Biochemical analysis of a dimerization domain mutation in RetGC-1 associated with dominant cone–rod dystrophy. Proc Natl Acad Sci USA 96:9039–9044.

Watanabe S-I, Matthews G (1988) Regional distribution of cGMP-activated ion channels in the plasma membrane of the rod photoreceptor. J Neurosci 8:2334–2337.

Wilkie SE, Newbold RJ, Deery E, Walker CE, Stinton I, Ramamurthy V, Hurley JB, Bhattacharya SS, Warren MJ, Hunt DM (2000) Functional characterization of missense mutations at codon 838 in retinal guanylate cyclase correlates with disease severity in patients with autosomal dominant cone–rod dystrophy. Hum Mol Genet 9:3065–3073.

Wilkie SE, Li Y, Deery EC, Newbold RJ, Garibaldi D, Bateman JB, Zhang H, Lin W, Zack DJ, Bhattacharya SS, Warren MJ, Hunt DM, Zhang K (2001) Identification and functional consequences of a new mutation (E155G) in the gene for GCAP1 that causes autosomal dominant cone dystrophy. Am J Hum Genet 69:471–480.

Woodford BJ, Chen J, Simon MI (1994) Expression of rhodopsin promoter transgene product in both rods and cones. Exp Eye Res 58:631–635.

Woodruff ML, Sampath AP, Matthews HR, Krasnoperova NV, Lem J, Fain GL (2002) Measurement of cytoplasmic calcium concentration in the rods of wild-type and transducin knock-out mice. J Physiol (Lond) 542:843–854.

Woodruff ML, Wang Z, Chung HY, Redmond TM, Fain GL, Lem J (2003) Spontaneous activity of opsin apoprotein is a cause of Leber congenital amaurosis. Nat Genet 35:158–164.